Microvascular Research 162 (2025) 104862

Contents lists available at ScienceDirect

Microvascular Research

journal homepage: www.elsevier.com/locate/ymvre

Assessing coronary microvascular dysfunction in refractory no-reflow: Insights from dynamic myocardial perfusion scintigraphy and cardiac MRI☆

Stanislav Dil *, Vyacheslav Ryabov, Leonid Maslov, Olga Mochula, Andrey Mochula, Maria Kercheva, Konstantin Zavadovsky, Evgeny Vyshlov

Cardiology Research Institute, Tomsk National Research Medical Center, Russian Academy of Sciences, Tomsk, Russia

ARTICLE INFO

Keywords:
Myocardial infarction
Refractory no-reflow phenomenon
Microvascular obstruction
Dynamic SPECT
Cardiac MRI

ABSTRACT

Background: Refractory no-reflow correlates with worse outcomes, including larger infarct sizes, impaired ventricular function, and higher mortality rates, despite advances in percutaneous coronary intervention (PCI). Microvascular obstruction (MVO) and increased left ventricular end-diastolic pressure (LVEDP) are implicated in the pathogenesis, potentially exacerbating ischemic injury and limiting myocardial recovery. While pressure-wire–derived indices such as the Index of Microcirculatory Resistance (IMR) have been validated against MRI-defined MVO in STEMI populations, their invasive nature and procedural complexity limit broad adoption. In contrast, combining dynamic SPECT and cardiac MRI enables a comprehensive non-invasive functional-structural evaluation of coronary microvascular function in refractory no-reflow.

Methods: This study is a post hoc analysis of a larger randomized controlled trial (RCT) evaluating the efficacy and safety of intracoronary epinephrine in patients with refractory no-reflow post-PCI (ClinicalTrials.gov NCT04573751). We evaluated global coronary flow metrics (RMBF, SMBF, gRFI) derived from SPECT and assessed structural markers of microvascular injury (infarct size, MVO) on MRI. Echocardiographic estimations of LVEDP were also analyzed.

Results: Dynamic SPECT revealed suboptimal stress myocardial blood flow in most patients, highlighting microvascular impairment. Elevated estimated LVEDP was significantly correlated with indexed MVO (rs = 0.678, $p = 0.001$). Traditional flow reserve metrics showed limited sensitivity, whereas global relative flow increase (gRFI) showed a statistically significant correlation with MVO, highlighting its added value in detecting stress-induced perfusion abnormalities. Given the small sample and potential outlier influence, this observation should be considered hypothesis-generating.

Conclusion: Our findings support that functional impairments—particularly elevated LVEDP and reduced gRFI—are associated with refractory no-reflow. In particular, gRFI may serve as a promising non-invasive marker of microvascular dysfunction, complementing structural imaging. None-theless, further validation in larger cohorts is needed. This study advocates for refined multimodal imaging strategies and tailored therapeutic approaches targeting dynamic microvascular disturbances to improve outcomes in refractory no-reflow.

1. Introduction

The no-reflow phenomenon, defined as the failure to restore adequate myocardial perfusion despite successful mechanical reperfusion of an occluded coronary artery, remains a critical challenge in optimizing outcomes for acute myocardial infarction (AMI) patients (Ibanez et al., 2018). Refractory no-reflow is particularly associated with larger infarct sizes, impaired left ventricular function, and increased rates of heart failure and mortality, even in the era of advanced percutaneous coronary intervention (PCI) (Ciofani et al., 2021; Annibali et al.,

☆ Tweet
"Novel insights into coronary microvascular dysfunction in refractory no-reflow using dynamic SPECT and cardiac MRI. Elevated LVEDP linked to microvascular obstruction highlights potential therapeutic targets. #Cardiology #NoReflow #CVD"

* Corresponding author at: Cardiology Research Institute, Tomsk National Research Medical Center, Russian Academy of Sciences, Kiyevskaya 111a, Tomsk, Russia.
E-mail address: dsv@cardio-tomsk.ru (S. Dil).

https://doi.org/10.1016/j.mvr.2025.104862
Received 18 June 2025; Received in revised form 14 August 2025; Accepted 18 August 2025
Available online 20 August 2025

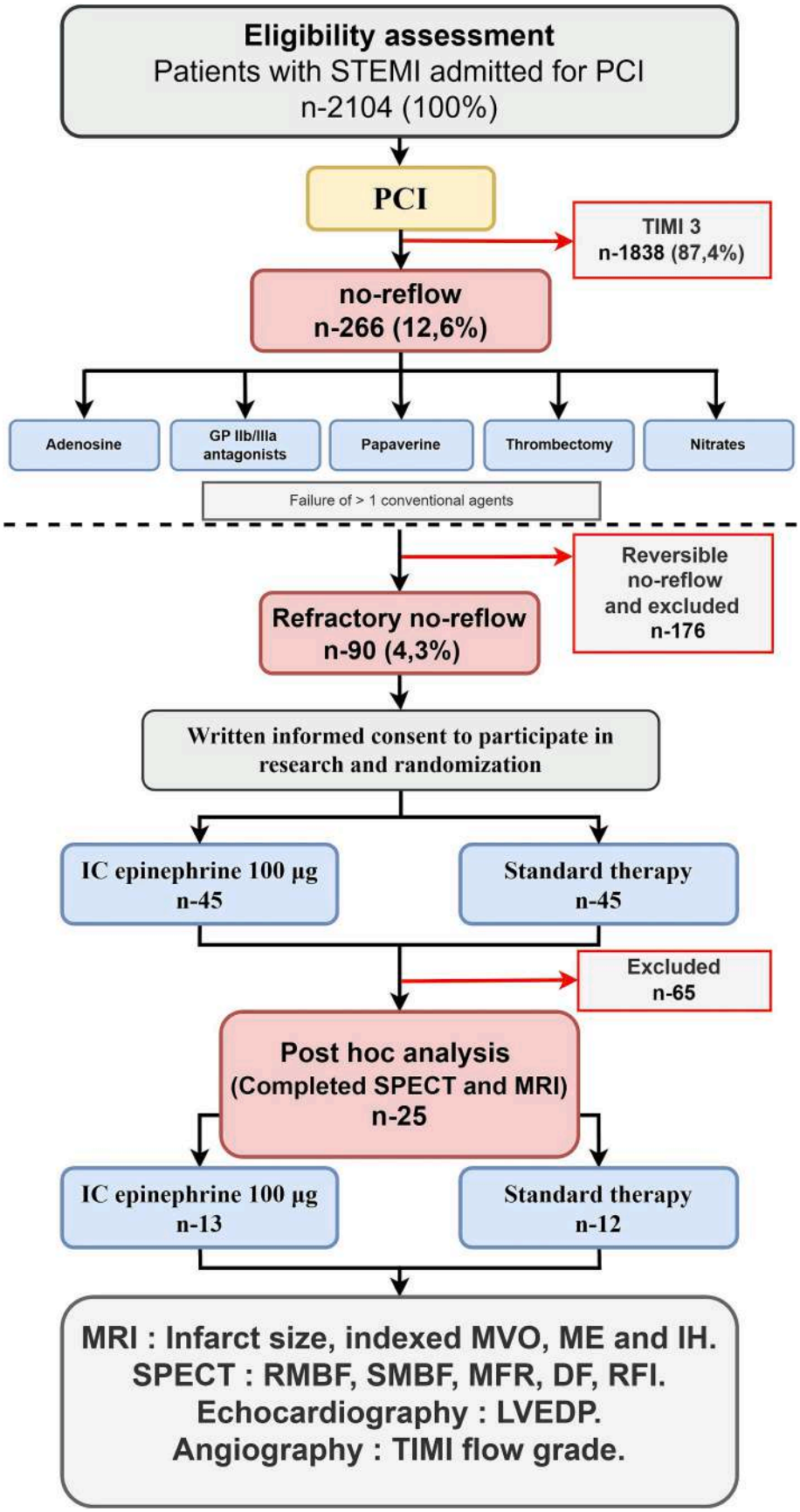

(caption on next page)

Fig. 1. Study design. DF — Difference Flow; GP — Glycoprotein; HR — Heart Rate; IC — Intracoronary; IH — Intramyocardial Hemorrhage; LVEDP — Lleft Ventricular End-Diastolic Pressure; MACE — Major Adverse Cardiovascular Events; ME — Myocardial Edema; MFR — Myocardial Flow Reserve; MRI — Magnetic Resonance Imaging; MVO — MicroVascular Obstruction; PCI — Percutaneous Coronary Intervention; RFI — Relative Flow Increase; RMBF — Rest Myocardial Blood Flow; SBP — Systolic Blood Pressure; SMBF — Stress Myocardial Blood Flow; SPECT — Single-Photon Emission Computerized Tomography; STEMI — ST Elevation Myocardial Infarction; TIMI — Thrombolysis in Myocardial Infarction.

2022; Hausenloy et al., 2017; Vyshlov et al., 2024; Galli et al., 2024).

The underlying mechanisms of no-reflow include microvascular obstruction (MVO), endothelial dysfunction, inflammation, and increased extravascular compression (Allencherril et al., 2019; Kaul et al., 2022; Ryabov et al., 2024a; Ryabov et al., 2023; de Waha et al., 2017; van Kranenburg et al., 2014). Cardiac magnetic resonance imaging (MRI) is currently the gold standard for assessing MVO and infarct characteristics, offering high-resolution structural evaluation (Kloner, 2017; Reinstadler et al., 2019; Robbers et al., 2013; Liu et al., 2021). Invasive pressure-wire indices, such as the Index of Microcirculatory Resistance (IMR), have been validated against MRI-defined MVO and long-term outcomes in STEMI, but their procedural complexity limits widespread adoption in routine practice; this underscores the need for non-invasive structural–functional approaches (Scarsini et al., 2021).

However, MRI provides a largely static assessment of myocardial tissue. In contrast, dynamic single-photon emission computed tomography (SPECT) allows quantitative evaluation of stress-induced myocardial blood flow, enabling a functional perspective on coronary microvascular reserve (Vorobeva et al., 2022; Kapur and O'Neill, 2019; Azzalini et al., 2022). This distinction is particularly important in refractory no-reflow, where dynamic disturbances of microvascular perfusion may not be fully reflected in conventional imaging. Elevated left ventricular end-diastolic pressure (LVEDP), a marker of diastolic dysfunction and wall stress, may further compromise microvascular flow and contribute to persistent perfusion defects (Azzalini et al., 2022). While LVEDP has been extensively studied in STEMI, its interaction with imaging-defined MVO and perfusion parameters remains insufficiently explored.

To date, no studies have provided an integrated structural–functional analysis of coronary microvascular dysfunction in patients with refractory no-reflow. Moreover, the potential role of novel perfusion metrics—such as global relative flow increase (gRFI) derived from dynamic SPECT—as correlates of MVO severity has not been previously investigated.

This study addresses this gap by performing a multimodal imaging analysis in a highly selected STEMI population with refractory no-reflow, combining cardiac MRI and dynamic SPECT. By correlating functional SPECT-derived flow indices with MRI-defined MVO, we aim to identify novel parameters that reflect the complexity of microvascular dysfunction beyond traditional metrics.

1.1. Study objective

The aim of this study is to assess the relationship between myocardial perfusion parameters obtained by dynamic SPECT and structural indicators of microvascular damage evaluated by MRI in patients with refractory no-reflow following STEMI. Special attention is given to the potential utility of gRFI as a novel marker of functional microvascular impairment, and its correlation with MVO volume. Additionally, we explore non-invasive echocardiographic estimates of LVEDP as a potential contributor to impaired microcirculation.

2. Materials and methods

2.1. Study design and setting

This analysis is a post hoc evaluation of data obtained from a single-center prospective randomized controlled interventional study titled "Efficiency and Safety of Intracoronary Epinephrine Administration in ST-Elevation Myocardial Infarction Patients with Refractory Coronary No-reflow" (Ryabov et al., 2024b; Dil et al., 2022). This trial was prospectively registered at ClinicalTrials.gov (NCT04573751) (ClinicalTrials.gov, n.d.). The primary objective of the main study was to assess the efficacy and safety of intracoronary epinephrine in patients with refractory no-reflow following emergency PCI.

Among the 2104 STEMI patients who underwent emergency PCI at the Cardiology Research Institute between December 2020 and March 2024, 266 patients (12.6 %) developed no-reflow, and 90 (4.6 %) were identified as having refractory no-reflow. All patients provided written informed consent upon hospital admission as part of the standard protocol for STEMI management, including consent for PCI and subsequent diagnostic and therapeutic procedures, in accordance with institutional ethical standards.

For the purposes of this post hoc analysis, only those patients who completed the full diagnostic protocol—including both dynamic SPECT and cardiac MRI—were selected. As a result, a final cohort of 25 patients was included, while the remaining 65 patients were excluded due to an incomplete set of diagnostic investigations. The reasons for exclusion (detailed in Appendix, Table 1) included: absolute contraindications to stress testing (e.g., left ventricular apical aneurysm or recurrent life-threatening arrhythmias), technical issues resulting in inadequate image quality, or clinical deterioration (including transfer to respiratory care unit due to COVID-19). In several cases, only partial diagnostic data (either SPECT or MRI) were available and deemed non-diagnostic.

In summary, the cohort of 25 patients represents those in whom the complete diagnostic protocol was successfully performed and yielded satisfactory image quality. A comparative analysis of included and excluded patients (Appendix, Table 2) showed that the only significant difference was a higher prevalence of type 2 diabetes mellitus in the excluded cohort (55.4 % vs. 32.0 %, $p = 0.047$). Additionally, there was a trend toward a lower use of glycoprotein IIb/IIIa inhibitors in excluded patients (41.5 % vs. 64.0 %, $p = 0.064$). The study design and patient selection process leading to the final cohort are illustrated in Fig. 1.

2.2. Refractory no-reflow definition and treatment groups

All patients underwent selective coronary angiography using the SIEMENS ARTIS ZEE FLOOR system. The no-reflow phenomenon was defined as TIMI flow <3 in the infarct-related artery after stent deployment, excluding mechanical complications such as dissection or acute thrombosis. No-reflow was considered refractory when it persisted despite intracoronary bolus administration of nitroglycerin (200–400 μg), adenosine (10–20 μg), or papaverine (10–20 mg), or intravenous administration of glycoprotein IIb/IIIa inhibitors (e.g., tirofiban 25 μg/kg, eptifibatide 180 μg/kg) in body weight–adjusted doses.

The use of vasodilators and/or IIb/IIIa inhibitors as initial therapy prior to randomization was left to the discretion of the interventional cardiologist, reflecting real-world variability in emergency management. Glycoprotein IIb/IIIa inhibitors were included in the definition of pharmacologic refractoriness due to their recognized adjunctive role in managing microvascular obstruction and thrombotic burden, despite differing mechanisms of action from vasodilators.

Upon confirmation of refractory no-reflow, patients were randomized using a simple randomization method into two groups:

- Group 1 received intracoronary epinephrine (100 μg via guiding catheter into the infarct-related artery);

Table 1
Clinical and anamnestic characteristics of patients.

Indicator	All	Epinephrine	Control	p
	n-25	n-13	n-12	
Age, years	63.2 (±11.7)	63.9 (±12.1)	62.6 (±11.8)	0.794
Male, n (%)	19 (76.0)	10 (76.9)	9 (75.0)	0.910
Hypertensive heart disease, n (%)	23 (92.0)	13 (100)	10 (83.3)	0.125
Smoking, n (%)	15 (60.0)	8 (61.5)	7 (58.3)	0.870
Body mass index, kg/m^2	29.3 (±4.3)	28.3 (±5.2)	30.3 (±3.1)	0.269
Type 2 diabetes mellitus, IGT, n (%)	8 (32.0)	4 (30.8)	4 (33.3)	0.891
Dyslipidemia, n (%)	20 (80.0)	10 (76.9)	10 (83.3)	0.689
Heredity, n (%)	10 (40.0)	7 (53.9)	3 (25.0)	0.141
History of angina pectoris, n (%)	4 (16.0)	2 (15.4)	2 (16.7)	0.930
History of prior MI, n (%)	2 (8.0)	2 (15.4)	0 (0)	0.157
Peripheral artery disease, n (%)	19 (76.0)	11 (84.6)	8 (66.7)	0.294
History of stroke, n (%)	1 (4.0)	1 (7.7)	0 (0)	0.327
AF, n (%)	3 (12.0)	2 (15.4)	1 (8.3)	0.588
Time from the onset of ACS symptoms, min	240.0 (160.0;370.0)	240.0 (160.0;540.0)	240.0 (155.0;310.0)	0.384
Thrombolytic therapy, n (%)	5 (20.0)	2 (15.4)	3 (25.0)	0.548
Laboratory data upon admission:				
GFR (CKD-EPI), ml/min/1.73 m2	63.6 (±13.1)	67.7 (±12.5)	59.1 (±12.7)	0.102
Leukocyte count 10^9/L	10.3 (8.5; 13.8)	8.7 (8.1; 12.6)	11.8 (10.1; 14.1)	0.201
Erythrocyte sedimentation rate, mm/h	12.0 (10.0; 19.0)	11.0 (7.0; 24.0)	15.0 (11.0; 18.5)	0.497
C-reactive protein, mg/l	21.2 (13.0; 37.0)	25.8 (14.6; 38.7)	21.2 (11.3; 28.4)	0.545
Platelet count 10^9/L	233.0 (184.0314.0)	258.0 (210.0314.0)	213.0 (183.5290.0)	0.480
Glucose, mmol/l	9.4 (7.5 12.1)	9.4 (±2.4)	11.2 (±3.8)	0.104
Cholesterol, mmol/l	5.2 (±1.1)	4.9 (±1.2)	5.6 (±0.9)	0.102
Triglycerides, mmol/l	1.7 (1.1; 3.0)	1.4 (1.0; 1.9)	2.2 (1.3; 3.4)	0.165
AHF grade according to the Killip scale upon admission:				
Killip I, n (%)	21 (84.0)	11 (84.6)	10 (83.4)	0.930
Killip II, n (%)	1 (4.0)	0 (0)	1 (8.3)	0.288
Killip III, n (%)	2 (8.0)	1 (7.7)	1 (8.3)	0.953
Killip IV, n (%)	1 (4.0)	1 (7.7)	0 (0)	0.327
P2Y12 inhibitors:				
Cloridogrel, n (%)	10 (40.0)	6 (46.2)	4 (33.3)	0.513
Ticagrelor, n (%)	13 (52.0)	6 (46.2)	7 (58.3)	0.543
Prasugrel, n (%)	2 (8.0)	1 (7.6)	1 (8.4)	0.327
Parameters for PCI:				
Residual coronary artery stenosis >50 %, n (%)	11 (44.0)	6 (46.2)	5 (41.7)	0.821
Direct stenting, n (%)	3 (12.0)	2 (15.4)	1 (8.3)	0.588
Infarction related coronary artery:				
Proximal LAD, n (%)	6 (24.0)	4 (30.8)	2 (16.7)	0.645
Mid LAD, n (%)	5 (20.0)	3 (23.1)	2 (16.7)	0.788
Distal LAD, n (%)	4 (16.0)	1 (7.7)	3 (25.0)	0.322
Diagonal branch of LAD, n (%)	3 (12.0)	1 (7.7)	2 (16.7)	0.593
Proximal LCx, n (%)	1 (4.0)	0 (0.0)	1 (8.3)	0.999
OM branch of LCx, n (%)	1 (4.0)	1 (7.7)	0 (0.0)	0.999
Proximal RCA, n (%)	3 (12.0)	2 (15.3)	1 (8.3)	0.593
Posterior descending artery, n (%)	2 (8.0)	1 (7.7)	1 (8.3)	0.571
Localization of infarction:				
Anteroseptal, n (%)	6 (24.0)	4 (30.8)	2 (16.7)	0.645
Anterior, n (%)	6 (24.0)	4 (30.8)	2 (16.7)	0.645
Anterolateral, n (%)	4 (16.0)	1 (7.7)	3 (25.0)	0.322
Lateral, n (%)	3 (12.0)	1 (7.7)	2 (16.6)	0.593
Inferior, n (%)	6 (24.0)	3 (23.0)	3 (25.0)	0.999
No-reflow treatment methods:				
Thrombaspiration, n (%)	12 (48.0)	5 (38.5)	7 (58.3)	0.219
Glycoprotein IIb/IIIa inhibitors, n (%)	16 (64.0)	8 (61.5)	8 (66.7)	0.562
Papaverine, n (%)	3 (12.0)	2 (15.4)	1 (8.3)	0.588
Nitroglycerine, n (%)	16 (64.0)	10 (76.9)	6 (50.0)	0.247
Adenosine, n (%)	3 (12.0)	1 (7.7)	2 (16.7)	0.439
TIMI blood flow after PCI before epinephrine administration:				
TIMI 0, n (%)	3 (12.0)	2 (15.4)	1 (8.3)	0.974
TIMI 1, n (%)	8 (32.0)	4 (30.8)	4 (33.3)	0.588
TIMI 2, n (%)	14 (56.0)	7 (53.8)	7 (58.4)	0.671

Variables are presented as mean and standard deviation (m ± SD) in case they are normally distributed, and as median (Me) and interquartile range (Q1; Q3) otherwise. Categorical variables were described by absolute and relative frequencies (%). Boldface denotes statistical significance.
Abbreviations: ACS – Acute Coronary Syndrome; AF – Atrial Fibrillation; AHF – Acute Heart Failure; CKD-EPI - Chronic Kidney Disease Epidemiology Collaboration Formula; CRP - C-Reactive Protein; ESR - Erythrocyte Sedimentation Rate; GFR – Glomerular Filtration Rate; IGT - Impaired Glucose Tolerance; LAD - Left Anterior Descending; LCX - Circumflex Coronary Artery; OM - Obtuse Marginal; PCI — Percutaneous Coronary Intervention; RCA – Right Coronary Artery; TIMI - Thrombolysis In Myocardial Infarction.

- Group 2 (control group) received a second administration of a conventional agent, typically nitroglycerin or IIb/IIIa inhibitor, as per operator judgment.

The detailed protocol for epinephrine preparation and administration is described in our prior publication (Ryabov et al., 2024b).

2.3. Echocardiography and LVEDP estimation

All patients underwent transthoracic echocardiography twice: within 1–2 days of admission and again on days 7–10 post-STEMI. Examinations were performed using the Philips CX50 system (s5–1 transducer) by experienced echocardiographers blinded to clinical status and imaging results. Standard parasternal and apical views were acquired in accordance with ASE guidelines (Gottdiener et al., 2004). Left ventricular end-diastolic pressure (LVEDP) was estimated non-invasively using Doppler-derived E/e' ratio. Transmitral peak velocity during early diastole (E) and early diastolic mitral annular velocity (e') were measured, and values were classified as follows: E/e' < 8: normal LVEDP (<12 mmHg), E/e' 8–15: indeterminate LVEDP (12–18 mmHg), E/e' ≥ 15: elevated LVEDP (≥18 mmHg) (Nagueh et al., 2016).

2.4. Cardiac MRI protocol

Cardiac MRI was performed on days 5 ± 2 post-STEMI, prior to hospital discharge, using a 1.5-T scanner (Vantage Titan, Toshiba). Cine

Table 2
Results of examination and treatment.

Indicator	All	Epinephrine	Control	p
	n-25	n-13	n-12	
Laboratory data:				
Troponin I on admission, ng/ml	0.4 (0.1; 1.8)	0.1 (0.1; 1.8)	0.8 (0.1;1.6)	0.605
Peak troponin I level, ng/ml	19.7 (6.1;25.0)	19.7 (9.8;25.0)	20.1 (4.7;36.1)	0.807
CPK - MV upon admission, units/l	31.0 (25.0;45.0)	31.0 (26.0;43.0)	31.1 (22.8;82.1)	0.724
Peak level of CPK - MV, units/l	143.8 (48.5;272.5)	141.8 (44.5;271.5)	162.8 (74.0;273.0)	0.570
Instrumental data:				
Achieving TIMI 3, n (%)	9 (36.0)	6 (46.2)	3 (25.0)	0.271
Resolution of ST elevation >50 %, n (%)	16 (64.0)	11 (84.6)	5 (41.7)	0.025
Hemodynamic parameters and complications of PCI:				
SBP before treatment, mmHg	123.6 (±22.3)	126.2 (±22.4)	120.7 (±22.9)	0.544
SBP after treatment, mm Hg	133.8 (±19.3)	143.9 (±12.3)	122.8 (±19.9)	0.004
DBP before treatment, mm Hg	75.8 (±11.7)	75.2 (±9.1)	76.4 (±14.5)	0.806
DBP after treatment, mm Hg.	81.1 (±9.5)	84.7 (±6.5)	77.3 (±10.9)	0.048
Heart rate before treatment	78.7 (±18.7)	81.9 (±16.8)	75.3 (±20.8)	0.396
Heart rate after treatment	80.0 (74.0;118.0)	113.9 (±35.6)	76.9 (±19.3)	0.004
Heart rhythm disorders, n (%)	6 (24.0)	5 (38.5)	1 (8.3)	0.080
Ventricular extrasystoles, n (%)	3 (12.0)	2 (15.4)	1 (8.3)	0.588
Atrial fibrillation, n (%)	2 (8.0)	2 (15.4)	0 (0)	0.157
Ventricular tachycardia, n (%)	4 (16.0)	2 (15.4)	2 (16.7)	0.930
Echocardiographic indicators:				
LV EDV 1–2 days, ml	103.8 (±24.9)	103.0 (±26.1)	104.7 (±24.6)	0.871
LV ESV 1–2 days, ml	52.0 (±14.4)	49.6 (±13.2)	54.5 (±15.7)	0.408
LVEF 1–2 days, %	50.0 (±7.3)	51.5 (±9.2)	48.5 (±6.5)	0.318
WMSI 1–2 days	1.5 (±0.3)	1.5 (±0.4)	1.6 (±0.3)	0.382
E/e` 1–2 days	8.6 (7.4;11.3)	8.7 (7.8;12.4)	8.3 (7.3;9.4)	0.446
LV EDV 7–10 days, ml	114.0 (±26.7)	112.5 (±25.1)	115.5 (±29.4)	0.788
LV ESV 7–10 days, ml	51.7 (±5.2)	50.2 (±12.1)	58.0 (±17.1)	0.200
LVEF 7–10 days, %	51.0 (48.0;54.0)	53.0 (49.0;54.0)	49.5 (47.5;52.5)	0.157
WMSI 7–10 days	1.5 (±0.3)	1.5 (±0.2)	1.5 (±0.3)	0.768
E/e` 7–10 days	9.5 (8.6;14.6)	9.4 (8.7;14.6)	9.6 (8.4;14.0)	0.957
Normal LVEDP (<12 mmHg), n (%)	4 (16.0)	2 (15.4)	2 (16.7)	0.930
Indeterminate LVEDP (12–18 mmHg), n (%)	15 (60.0)	8 (61.5)	7 (58.3)	0.870
Elevated LVEDP (≥18 mmHg) n (%)	6 (24.0)	3 (23.1)	3 (25.0)	0.911
Hospital mortality, n (%)	1 (4.0)	0 (0)	1 (8.3)	0.288
MACE events within 30 days, n (%)	4 (16.0)	1 (7.7)	3 (25.0)	0.323

Abbreviations: ACS – Acute Coronary Syndrome; AF – Atrial Fibrillation; AHF – Acute Heart Failure; CKD-EPI - Chronic Kidney Disease Epidemiology Collaboration Formula; CRP - C-Reactive Protein; DBP – Diastolic Blood Pressure; ESR - Erythrocyte Sedimentation Rate; GFR – Glomerular Filtration Rate; IGT - Impaired Glucose Tolerance; LAD - Left Anterior Descending; LCX - Left CircumfleX artery; MACE – Major Adverse Cardiovascular Events; PCI — Percutaneous Coronary Intervention; RCA – Right Coronary Artery; SBP - Systolic Blood Pressure; TIMI - Thrombolysis In Myocardial Infarction.

Table 3
MRI indicators.

Indicator	All	Epinephrine	Control	p
	n-25	n-13	n-12	
LV mass, g	142.0 (131.1; 161.4)	148.9 (127.0;147.0)	137.0 (131.1;173.0)	0.861
LA volume, ml	75.4 (62.0; 94.8)	79.6 (67.2;99.0)	69.8 (61.1; 75.7)	0.307
LA area 4ch, cmˆ2	23.8 (20.7; 24.8)	24.3 (23.8;27.8)	22.2 (20.7;24.2)	0.178
T2 SI total enhanced mass, g	50.9 (±16.9)	50.9 (±16.1)	51.0 (±18.5)	0.983
T2 SI enhanced volume (rel), %	33.4 (±10.9)	34.0 (±12.2)	32.9 (±10.1)	0.820
LE total enhanced mass, g	24.7 (17.1; 30.9)	27.6 (16.4;30.9)	21.4 (18.6;33.1)	0.972
LE Enhanced volume (rel), %	13.9 (11.0; 18.5)	14.9 (11.8;19.4)	13.8 (9.6;17.3)	0.805
LE no-reflow mass, g	0.7 (0.3; 3.9)	0.5 (0.2; 2.5)	1.6 (0.4; 4.5)	0.291
LE no reflow (indexed MVO) %	0.6 (0.2; 2.4)	0.4 (0.1; 1.8)	1.8 (0.3; 2.6)	0.260
Salvaged area at risk, %	17.8 (±10.4)	20.8 (±13.1)	15.3 (±7.3)	0.250
Edema, n (%)	20 (80.0)	9 (69.3)	11 (91.7)	0.283
MVO, n (%)	20 (80.0)	10 (76.9)	10 (83.3)	0.329
IH, n (%)	17 (68.0)	8 (61.5)	9 (75.0)	0.916

Abbreviations: IH - Intramyocardial Hemorrhage; LA – Left Atrial; LE – Late Enhancement; LV – Left Ventricular; MRI — Magnetic Resonance Imaging; MVO - Microvascular Obstruction; SI – Signal Intensity.

imaging, T2-weighted sequences, and contrast-enhanced late gadolinium enhancement (LGE) were obtained to assess infarct size, myocardial edema, microvascular obstruction (MVO), and intramyocardial hemorrhage. LGE images were processed using CVI42 software (v5.1.1, Circle Cardiovascular Imaging), and MVO was defined as a hypoenhanced region surrounded by hyperenhancement. Infarct size and MVO were indexed to total LV mass.

2.5. Dynamic SPECT imaging and flow quantification

Dynamic SPECT was performed on days 6–7 post-STEMI, when patients were clinically stable and eligible for pharmacological stress. A two-day rest–stress protocol was used on the Discovery NM/CT 570c hybrid system (GE Healthcare) equipped with cadmium-zinc-telluride (CZT) detectors. Rest study (day 1): low-dose CT for positioning, dynamic gated SPECT imaging for 12 min, followed by standard gated MPS after 60 min. Stress study (day 2): infusion of ATP (160 μg/kg/min for 4 min), radiotracer injection at peak hyperemia, followed by gated dynamic acquisition. SPECT data were processed on the Xeleris workstation using 4DM Reserve v.2015 and Corridor 4DM (INVIA, USA).

Quantitative parameters included: Rest myocardial blood flow (RMBF), Stress myocardial blood flow (SMBF), Myocardial flow reserve (MFR), Difference flow (DF), Relative flow increase (RFI = [SMBF − RMBF] / RMBF).

2.6. Endpoints and perfusion analysis

Primary imaging endpoints included infarct size and MVO volume (MRI), edema and hemorrhage (qualitative), and quantitative SPECT perfusion parameters (RMBF, SMBF, MFR, DF, RFI). Correlative analyses were conducted between MRI-derived MVO and SPECT-derived flow

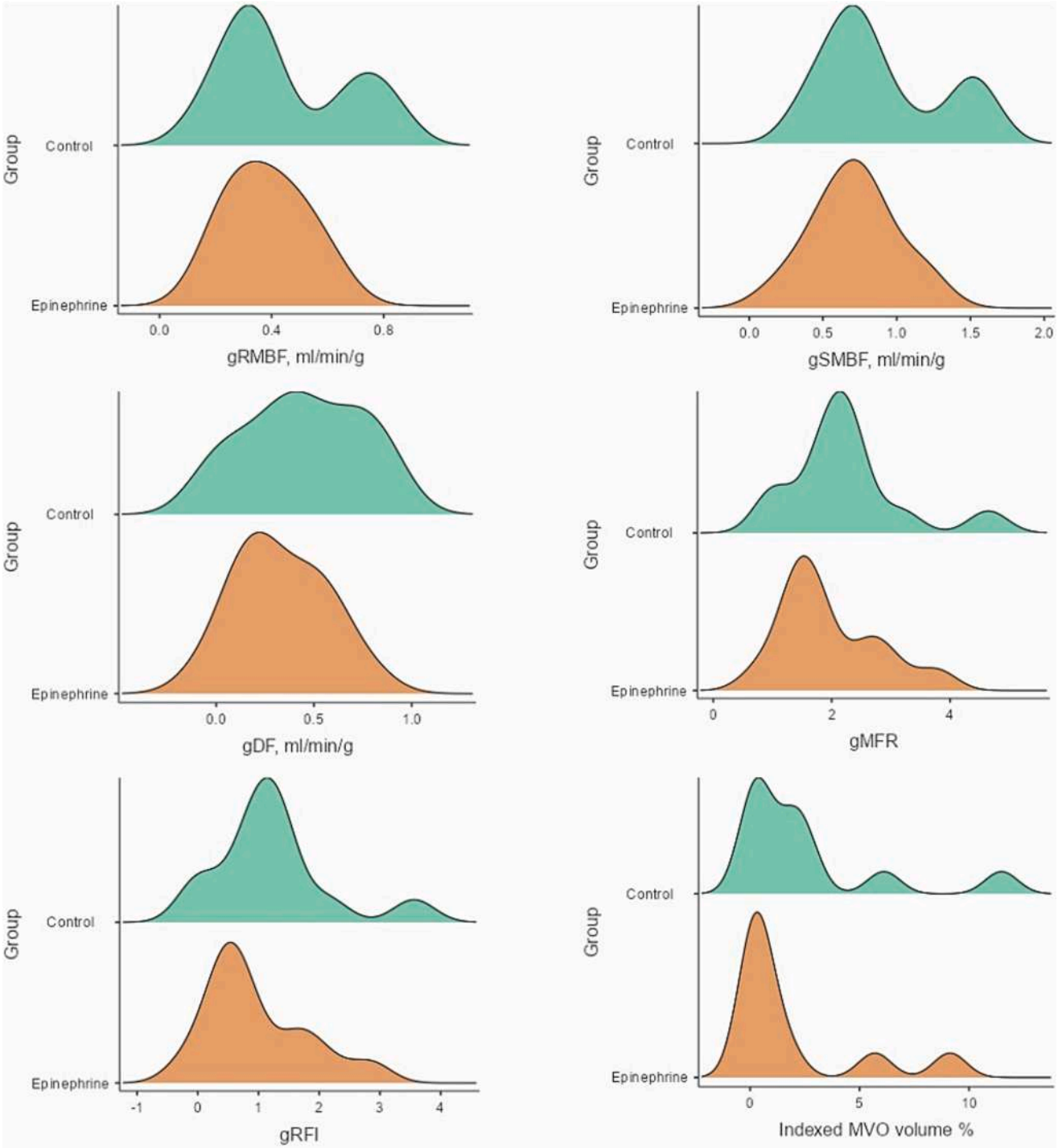

Fig. 2. Key global coronary flow metrics derived from dynamic SPECT, as well as the MVO index derived from MRI in each group. gDF – global Difference Flow; gMFR – global Myocardial Flow Reserve; MRI —Magnetic Resonance Imaging, gRFI - global Relative Flow Increase; gRMBF – global Resting Myocardial Blood Flow; gSMBF – global Stress Myocardial Blood Flow.

metrics, with specific focus on global relative flow increase (gRFI) as a potential indicator of functional microvascular impairment. In addition, LVEDP estimates and TIMI flow grades were included in the analysis to assess their relationship with structural and functional perfusion markers.

3. Statistical methods

The normality of the distribution of quantitative variables was assessed using the Shapiro-Wilk test. Variables with a normal distribution are presented as the mean and standard deviation (m ± SD), and those without a normal distribution are presented as the median (Me) and interquartile range (Q1; Q3). Categorical variables are described as absolute (n) and relative frequencies (i.e. in %). To compare normally distributed quantitative variables between two independent treatment groups, Student's *t*-test was used, while the Mann-Whitney *U* test was applied for non-normally distributed variables. Paired Student's t-test was employed to assess dynamic changes in normally distributed quantitative variables, and the Wilcoxon signed-rank test was used when normality was not observed. Categorical variables were compared

Table 4
Dynamic SPECT indicators.

Indicator	All	Epinephrine	Control	p
	n-25	n-13	n-12	
SMBF _LAD, ml/min/g	0.65 (0.54; 0.79)	0.64 (0.47; 0.77)	0.71 (0.58; 1.3)	0.253
SMBF _LcX, ml/min/g	0.97 (±0.44)	1.06 (0.59; 1.11)	0.94 (0.68; 1.50)	0.703
SMBF _RCA, ml/min/g	0.83 (±0.37)	0.77 (±0.33)	0.90 (±0.41)	0.376
Global SMBF, ml/min/g	0.80 (±0.35)	0.72 (0.52; 0.84)	0.76 (0.65; 1.28)	0.370
RMBF _LAD, ml/min/g	0.33 (0.28; 0.49)	0.33 (0.25; 0.44)	0.34 (0.30; 0.61)	0.514
RMBF _LcX, ml/min/g	0.53 (±0.26)	0.50 (±0.23)	0.57 (±0.29)	0.526
RMBF _RCA, ml/min/g	0.44 (±0.18)	0.43 (±0.16)	0.45 (±0.21)	0.753
Global RMBF, ml/min/g	0.35 (0.28; 0.50)	0.38 (±0.14)	0.45 (±0.23)	0.371
DF_LAD, ml/min/g	0.36 (±0.29)	0.29 (±0.23)	0.42 (±0.33)	0.260
DF_LcX, ml/min/g	0.44 (±0.35)	0.39 (±0.26)	0.49 (±0.42)	0.510
DF_RCA, ml/min/g	0.40 (±0.27)	0.35 (±0.25)	0.49 (±0.29)	0.321
Global DF, ml/min/g	0.39 (±0.27)	0.33 (±0.23)	0.45 (±0.29)	0.269
MFR _LAD	2.10 (±0.92)	1.93 (±0.85)	2.29 (±1.00)	0.345
MFR _LcX	1.83 (1.34; 2.57)	1.56 (1.33; 2.34)	1.90 (1.41; 2.59)	0.807
MFR _RCA	2.01 (1.36; 2.39)	1.96 (1.31; 2.27)	2.10 (1.76; 2.45)	0.399
Global MFR	2.09 (±0.89)	1.96 (±0.84)	2.23 (±0.96)	0.450
RFI_LAD	1.00 (±0.76)	0.93 (±0.86)	1.08 (±0.67)	0.635
RFI_LcX	0.80 (0.33; 1.58)	0.55 (0.33; 1.32)	0.88 (0.42; 1.59)	0.808
RFI_RCA	1.02 (0.39; 1.37)	0.94 (0.31; 1.26)	1.08 (0.74; 1.45)	0.430
Global RFI	1.09 (±0.89)	0.97 (±0.85)	1.22 (±0.94)	0.482

Abbreviations: DF - Difference Flow; LAD - Left Anterior Descending; LCX - Circumflex Coronary Artery; MFR - Myocardial Flow Reserve; RFI - Relative Flow Increase; RCA - Right Coronary Artery; RMBF - Resting Myocardial Blood Flow; SMBF - Stress Myocardial Blood Flow.

Table 5
Correlations between indexed MVO volume and myocardial flow in the overall cohort.

Indexed MVO volume %		
Global SMBF, ml/min/g	Spearman ρ(rho) *p*-value	0.0831 0.720
Global RMBF, ml/min/g	Spearman ρ(rho) p-value	−0.2512 0.273
Global MFR	Spearman ρ(rho) p-value	0.4132 0.063
Global DF, ml/min/g	Spearman ρ(rho) p-value	0.3081 0.175
Global RFI	Spearman ρ(rho) *p*-value	0.6261 0.002
E/e' 7–10 days	Spearman ρ(rho) p-value	0.6784 0.001

The data are presented as Spearman's rank correlation coefficients (ρ) and corresponding *p*-values.
Abbreviations: DF - Difference Flow; MFR - Myocardial Flow Reserve; MVO - MicroVascular Obstruction; RFI - Relative Flow Increase; RMBF - Resting Myocardial Blood Flow; SMBF - Stress Myocardial Blood Flow;

between two independent groups using Pearson's $\chi 2$ test or Fisher's exact test, depending on the expected frequencies. Correlation between the volume of MVO and relative coronary flow reserve was evaluated using Spearman's correlation coefficient. A critical significance level of 0.05 was applied for hypothesis testing.

4. Results

Baseline characteristics, including clinical history, laboratory findings, and MI profiles, were well-matched between groups, with no significant differences in age, gender, cardiovascular risk factors, comorbidities, infarct size, or location (Table 1).

There were no significant differences between groups regarding life-threatening arrhythmias or conduction disturbances. Transient increases in SBP, HR, and rhythm disturbances were observed in the epinephrine group, but they did not result in adverse outcomes or require therapeutic intervention (Table 2).

While no significant differences were found in enzymatic infarct size, a trend toward achieving TIMI 3 flow was observed in the epinephrine group, though this did not reach statistical significance. Notably, ST-segment resolution > 50 % post-PCI was significantly higher in the epinephrine group (78.0 % vs. 36.0 %, $p < 0.001$) (Table 2).

In our cohort, only 16 % of patients demonstrated a normal LVEDP (<12 mmHg) according to non-invasive assessment, with the remaining majority exhibiting elevated LVEDP. Echocardiographic evaluation of left ventricular ejection fraction (LVEF) within 1–2 days post-MI showed no statistically significant differences between groups, with mean values of 51.5 % (±9.2) in the epinephrine group and 48.5 % (±6.5) in the control group ($p = 0.318$). By days 7–10, LVEF remained slightly higher in the epinephrine group, recorded at 53.0 % (49.0; 54.0), compared to 49.5 % (47.5; 52.5) in the control group, although this difference did not reach statistical significance ($p = 0.157$). Across other echocardiographic parameters, no significant differences were observed between groups (Table 2).

The indexed MVO volume showed no significant differences between the groups: 0.4 % (0.1; 1.8) vs. 1.8 % (0.3; 2.6), respectively ($p = 0.250$). Similarly, there were no significant differences observed in indexed myocardial necrosis size: 14.9 % (11.8; 19.4) vs. 13.8 % (9.6; 17.3), $p = 0.805$; myocardial edema: 34.0 % (±12.2) vs. 32.9 % (±10.1), $p = 0.820$; salvaged area at risk: 20.8 % (±13.1) vs. 15.3 % (±7.3), $p = 0.250$; and the incidence of myocardial hemorrhage: 61.5 % vs. 75.0 %, $p = 0.916$. These values are summarized in Table 3 for further reference.

Key global myocardial flow metrics derived from dynamic SPECT, including global RMBF (gRMBF), global SMBF (gSMBF), global DF (gDF), global MFR (gMFR), global RFI (gRFI), as well as the MVO index derived from MRI, are presented for each group in the Fig. 2. No statistically significant differences in dynamic SPECT parameters were observed between the epinephrine and control groups (Table 4).

The analysis of myocardial flow metrics revealed that gRMBF was significantly reduced in both groups, with a median value of 0.35 ml/min/g (0.28; 0.50). Following pharmacological stress, gSMBF increased to 0.80 ml/min/g (±0.35), while still remaining suboptimal. The gMFR was measured at 2.09 (±0.89) (Table 4).

In the overall cohort, correlations between the MRI-derived MVO index and gRMBF (rs = −0.2512, $p = 0.273$), gSMBF (rs = 0.0831, $p = 0.720$), as well as gMFR (rs = 0.4132, $p = 0.063$), were not statistically significant (Table 5).

In the epinephrine group, no statistically significant correlations were found between the MVO index and gRMBF (rs = −0.3091, $p = 0.640$) or gSMBF (rs = 0.2612, $p = 0.511$). Similarly, in the control group, no significant correlations were observed between the MVO index and gRMBF (rs = −0.3462, $p > 0.545$) or gSMBF (rs = −0.2691, $p > 0.514$).

To provide a more accurate assessment of coronary vasculature response to stress, we calculated the global relative flow increase (gRFI) ((gSMBF − gRMBF) / gRMBF). Importantly, in the overall patient cohort, gRFI was found to be significantly correlated with the MVO index, as assessed by MRI (rs = 0.6261, $p = 0.002$) (Fig. 3). In the treatment group, the correlation between the MVO index and gRFI narrowly missed statistical significance (rs = 0.5697, $p = 0.087$). However, in the control group, the correlation between the MVO index and gRFI was slightly stronger and reached statistical significance (rs =

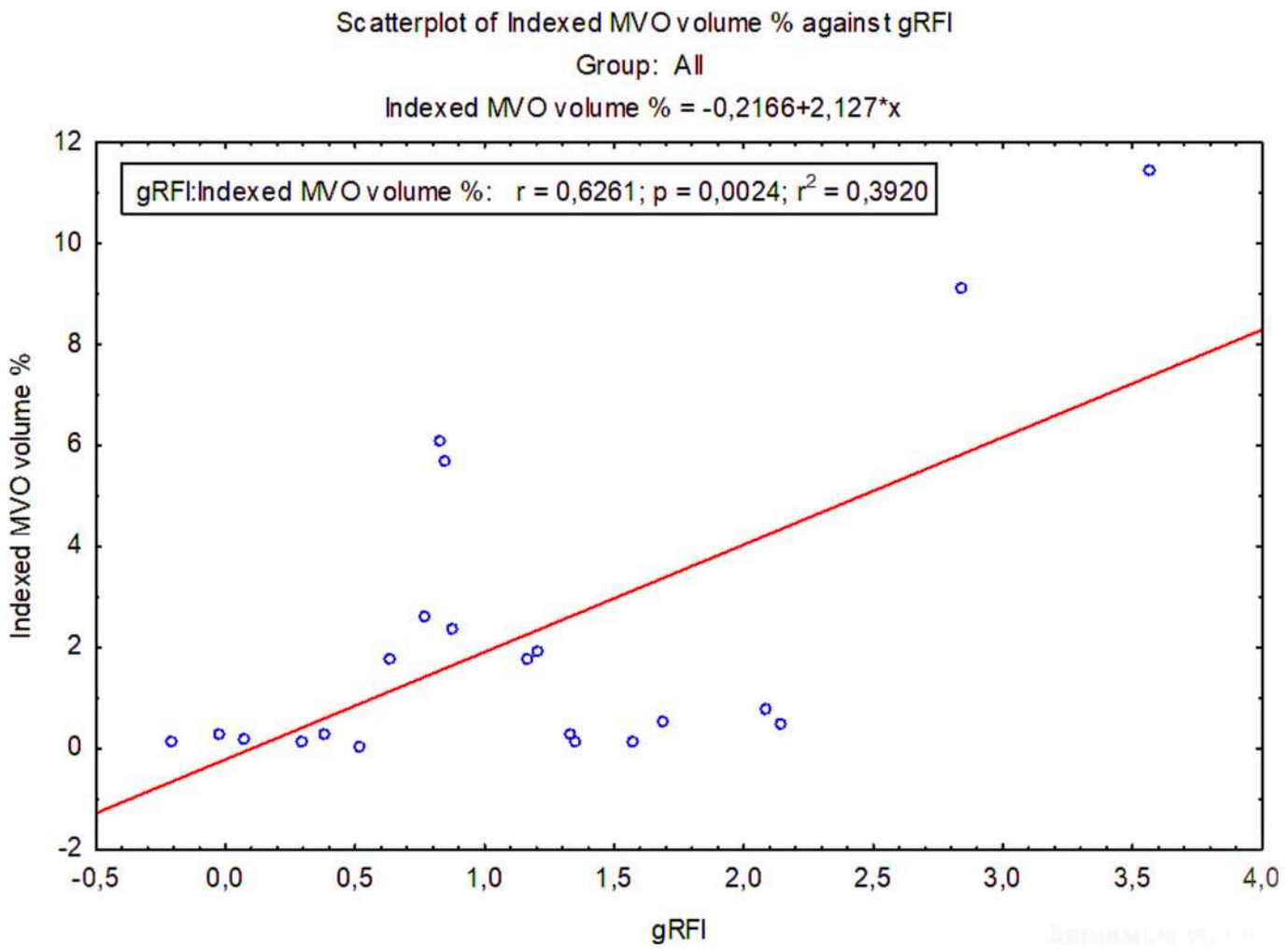

Fig. 3. Correlation Between gRFI and MVO Index in the Overall Patient Cohort. gRFI - Global Relative Flow Increase; MVO - MicroVascular Obstruction.

0.6654, $p = 0.025$) (Fig. 4).

Only 16 % of patients in the overall cohort exhibited normal LVEDP (<12 mmHg) based on non-invasive E/e' measurements. No significant differences in E/e' were observed between groups, either at 1–2 days or at 7–10 days. A significant positive correlation was identified between the E/e' ratio measured at 7–10 days and indexed microvascular obstruction (MVO) (rs = 0.6784, $p = 0.001$) (Fig. 5).

5. Discussion

The findings from our study, which uniquely combined dynamic SPECT and cardiac MRI, offer critical insights into coronary microvascular function in patients with refractory no-reflow. This multimodal approach fills a notable gap in current literature, as no previous studies have utilized this comprehensive combination to assess myocardial perfusion and myocardial reserve in this context. Previous studies have evaluated microvascular dysfunction using pressure-wire derived indices such as IMR, which correlate with MVO on MRI (Scarsini et al., 2021). However, our study focused on non-invasive imaging techniques applicable in real-world clinical settings. Our results, while multifaceted, provide several key considerations for the development of future therapeutic strategies targeting refractory no-reflow.

Although no significant differences were observed between the epinephrine and control groups in terms of key outcomes, it is important to emphasize that the primary goal of this analysis was not to evaluate the therapeutic efficacy of epinephrine, as this was addressed in a separate investigation. Instead, the focus of this sub-analysis was on the dynamics of myocardial blood flow in patients who underwent detailed multimodal imaging, particularly MRI and dynamic SPECT.

Assessing LVEDP is crucial for understanding microvascular function, and its potential role in predicting myocardial recovery requires further investigation. Only 16 % of patients demonstrated normal LVEDP (<12 mmHg) through non-invasive E/e' measurements, while the majority exhibited elevated levels, underscoring the prevalence of diastolic dysfunction in this cohort. A significant positive correlation was observed between E/e' measured at 7–10 days and indexed MVO (rs = 0.6784, $p = 0.001$), suggesting that higher ventricular filling pressures may be associated with greater degrees of microvascular obstruction. However, whether LVEDP serves as a predictor of adverse outcomes remains to be determined in future studies.

Interestingly, we identified a correlation between gRFI and the volume of MVO, as quantified by MRI. While this might initially seem counterintuitive—given that one would expect severe MVO to impair flow reserve—there is a plausible explanation. MRI is a static imaging modality that primarily captures structural and anatomical features at rest, without differentiating dynamic functional disturbances in the microcirculation. In contrast, dynamic SPECT assesses both rest and stress perfusion, offering insight into transient functional impairments such as vasospasm or endothelial dysfunction. These abnormalities may improve under pharmacological stress, potentially resulting in an exaggerated relative increase in perfusion.

To our knowledge, this is among the first exploratory reports to demonstrate a direct correlation between dynamic SPECT-derived gRFI and MRI-defined MVO in a STEMI population with refractory no-reflow.

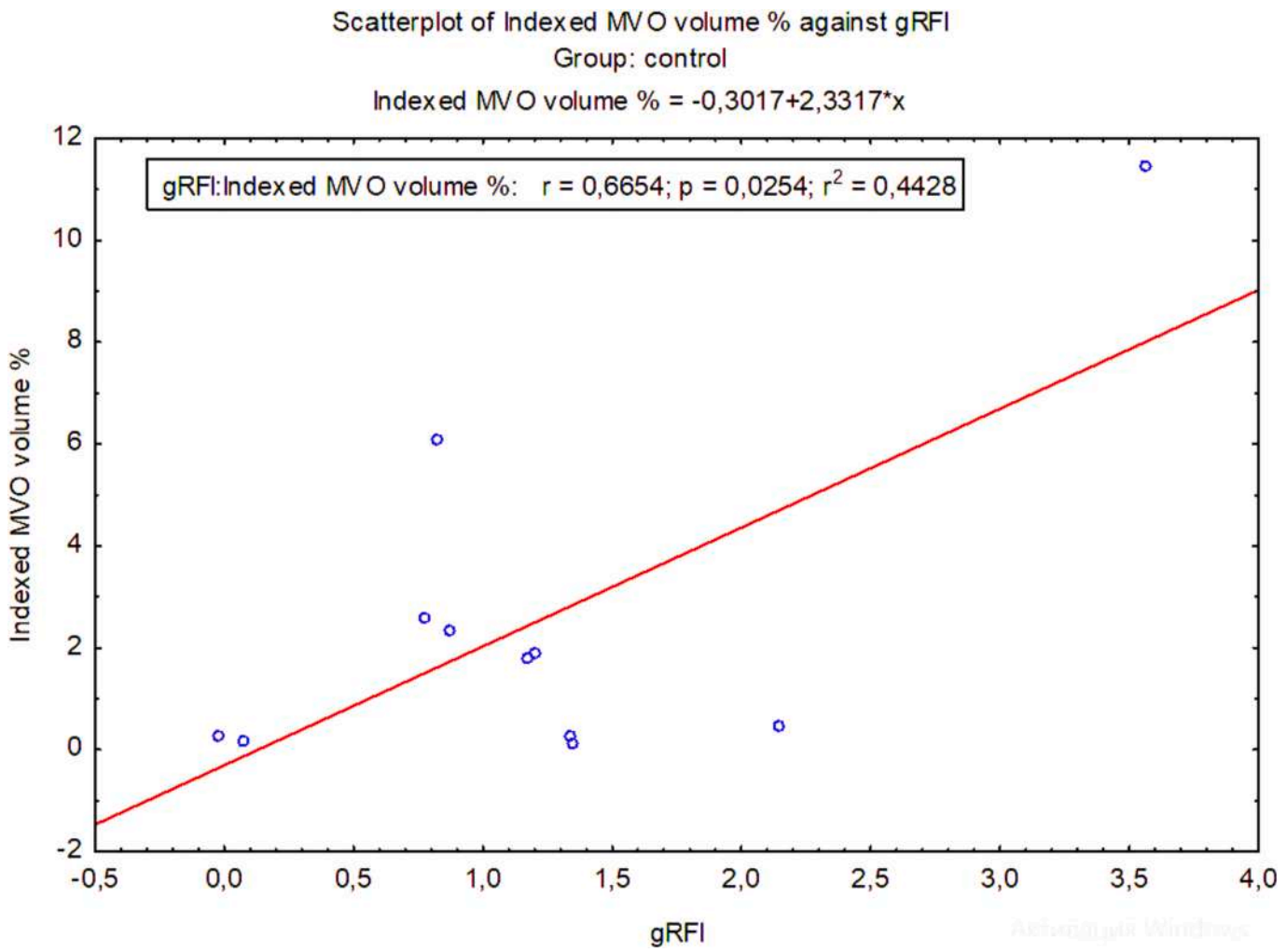

Fig. 4. Correlation Between gRFI and MVO Index in the Control. gRFI - Global Relative Flow Increase; MVO - MicroVascular Obstruction.

This functional marker may offer complementary information to anatomical imaging, although further studies are necessary to determine its consistency and reliability.

While absolute rest and stress MBF values were analyzed independently, their overlap across patients limited their discriminatory capacity. Traditional myocardial flow reserve (gMFR) also showed limited correlation with MVO. In contrast, gRFI—as a normalized flow ratio—better captured subtle impairments in coronary reserve. These findings support the hypothesis that dynamic stress-related flow indices, rather than absolute perfusion values, may provide deeper insight into the physiological mechanisms underlying the benefit of intracoronary adrenalin.

This observation raises the possibility that in patients with refractory no-reflow, microvascular dysfunction could involve functional disturbances, such as vasospasm or dynamic changes in vascular tone, to a greater extent than previously recognized. While this interpretation aligns with our data, it remains hypothesis-generating and highlights the need to re-evaluate the relative contributions of structural versus functional factors in microvascular pathology. If confirmed in future studies, these findings could support exploring therapeutic strategies aimed at modulating functional impairments in the microcirculation, which might offer clinical benefits in this patient population.

In summary, this study underscores the complexity of coronary microvascular dysfunction in refractory no-reflow. While structural changes like MVO may correlate with gRFI, absolute flow values may not consistently reflect these relationships. Our results emphasize the need for future research to refine imaging techniques, explore the temporal dynamics of microvascular dysfunction, and develop targeted therapies to optimize outcomes for patients with refractory no-reflow.

6. Study limitations

This study has several limitations. First, the exploratory nature of multiple correlation analyses (e.g., between LVEDP, gRFI, and MVO) increases the risk of type I errors due to the lack of correction for multiple comparisons. As this study included only 25 patients who completed both SPECT and MRI protocols, the risk of selection bias cannot be excluded. Although we identified statistically significant correlations, these findings—particularly involving the novel gRFI metric—require validation in larger, hypothesis-driven studies to confirm their clinical relevance and generalizability. Second, the small cohort size ($n = 25$) further restricts statistical power and precision, particularly in subgroup analyses. These limitations underscore the need for larger prospective studies to confirm our findings and refine the role of gRFI in clinical practice. Additionally, correlation analyses may be influenced by a few high-leverage observations, and results should be interpreted with caution.

7. Limitations of SPECT

While dynamic SPECT provides valuable insights into myocardial perfusion and coronary flow reserve, several limitations must be

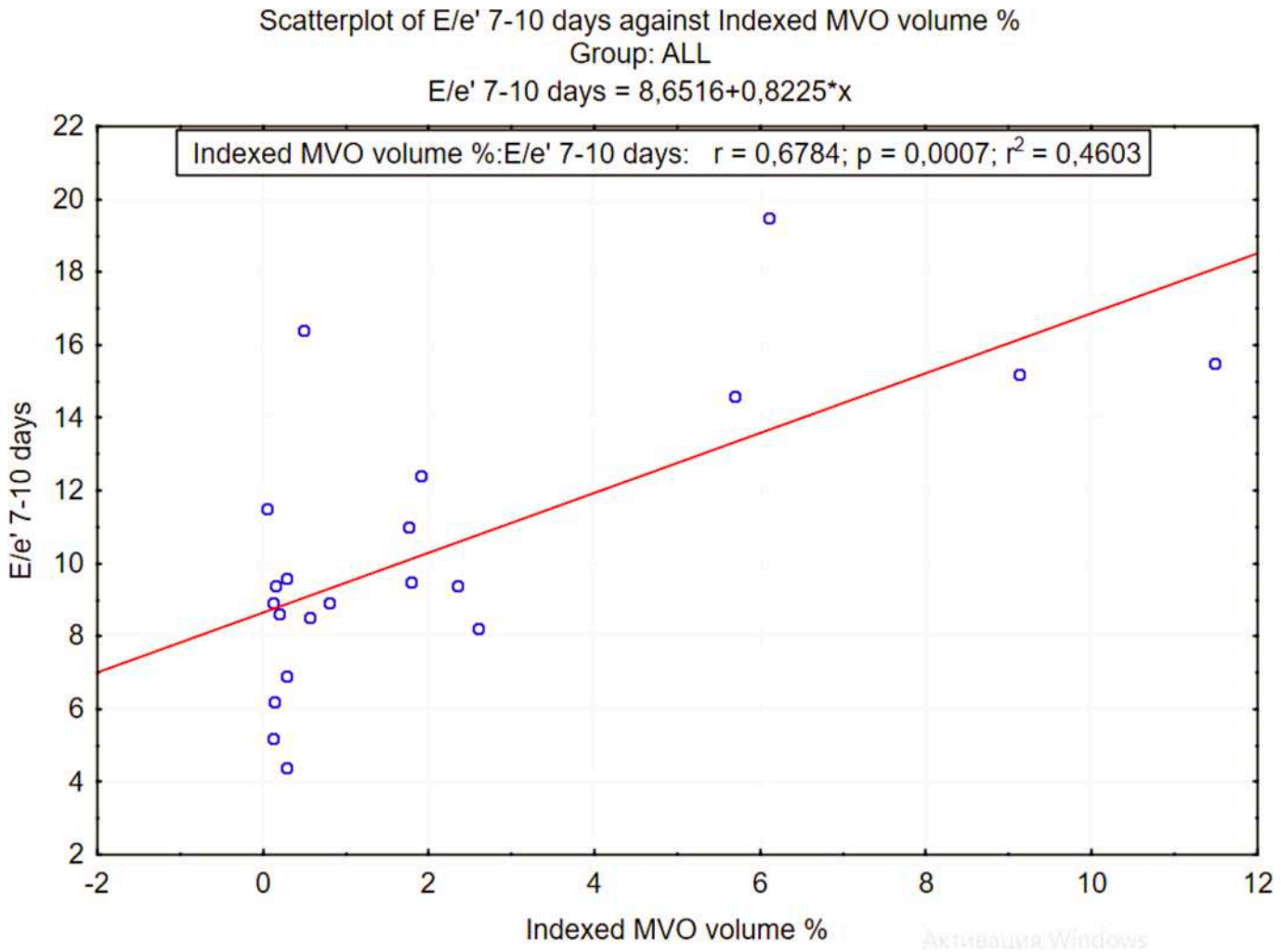

Fig. 5. Correlation Between LVEDP and MVO Index in the Overall Patient Cohort. MVO - MicroVascular Obstruction.

considered. Motion artifacts, partial volume effects, and variability in tracer uptake kinetics can introduce measurement variability. Additionally, the temporal resolution of dynamic SPECT is relatively low, which may limit its ability to capture rapid changes in myocardial blood flow. A key limitation is the underestimation of myocardial blood flow (MBF) values, particularly under stress conditions. This is primarily due to the non-linear relationship between 99mTc-MIBI retention and true blood flow, especially at high flow rates. This property of the tracer leads to systematic underestimation of MBF, affecting the accuracy of perfusion assessment. Despite these technical challenges, previous studies have demonstrated excellent inter-observer agreement in SPECT-based flow quantification (Agostini et al., 2018; Otaki et al., 2021), supporting its reliability. When combined with complementary imaging modalities such as cardiac MRI, dynamic SPECT remains a useful tool for assessing myocardial perfusion and flow reserve. In addition, the availability and cost of dynamic SPECT, as well as the need for pharmacological stress testing and post-processing, may limit its feasibility for routine implementation in acute STEMI care outside of specialized centers. Moreover, as this analysis was not pre-specified in the original trial design, the findings regarding gRFI should be interpreted as exploratory and hypothesis-generating.

8. Conclusion

This study provides new insights into the complex pathophysiology of coronary microvascular dysfunction in patients with refractory no-reflow, using a non-invasive multimodal imaging approach. While elevated LVEDP may contribute to microvascular compression, our findings suggest that static diastolic parameters alone may be insufficient to characterize dynamic perfusion disturbances. One of the most intriguing exploratory observations in our study was a correlation between gRFI and MRI-defined MVO. Although this finding requires validation, it may suggest a potential link between stress-induced microvascular function and structural myocardial injury. This suggests that gRFI may be a more sensitive marker of stress-induced microvascular dysfunction than traditional resting flow metrics or global myocardial flow reserve. These findings support the integration of functional and structural imaging modalities to assess coronary microcirculation in this high-risk population. Further studies with larger cohorts are warranted to validate the diagnostic and prognostic value of gRFI and refine patient stratification and therapeutic targeting in refractory no-reflow.

9. Clinical perspectives and impact on daily practice

The findings of this study offer critical insights into the management of patients with refractory no-reflow, a complication that significantly worsens outcomes in ST-elevation myocardial infarction (STEMI) despite timely percutaneous coronary intervention (PCI). Traditional markers such as TIMI flow grade or global myocardial flow reserve (gMFR) often fail to capture the complexity of microvascular dysfunction. Integration of functional flow indices such as gRFI may eventually

help tailor pharmacologic interventions, including the potential use of vasomodulators like epinephrine, in selected STEMI patients with microvascular dysfunction. These insights may aid clinicians in identifying patients who are more likely to benefit from targeted vasomodulatory therapy after PCI, potentially optimizing post-infarction recovery.

CRediT authorship contribution statement

Stanislav Dil: Writing – original draft, Methodology, Investigation, Formal analysis, Data curation, Conceptualization. **Vyacheslav Ryabov:** Writing – review & editing, Supervision, Conceptualization. **Leonid Maslov:** Writing – review & editing, Software, Methodology. **Olga Mochula:** Visualization, Software, Investigation. **Andrey Mochula:** Visualization, Software, Investigation. **Maria Kercheva:** Writing – review & editing, Software. **Konstantin Zavadovsky:** Visualization, Methodology, Conceptualization. **Evgeny Vyshlov:** Writing – review & editing, Supervision, Conceptualization.

Declaration of competing interest

The authors declare that they have no known competing financial interests or personal relationships that could have appeared to influence the work described in this article.

The work was carried out without the involvement of grants or financial support from public, non-profit and commercial organizations.

Appendix A

Table 1
Reasons for exclusion of patients ($n = 65$) from the main study.

Exclusion category	Number of patients	Comments
Did not complete both MRI and dynamic SPECT	(Agostini et al., 2018) patients	Patients who did not undergo either MRI or dynamic SPECT due to technical issues or absolute contraindications (e.g., severe arrhythmias or left ventricular apical aneurysm).
Completed MRI only (SPECT missing)	[30] patients	Patients excluded because they did not undergo dynamic SPECT, often due to clinical instability preventing stress testing, technical difficulties, or transfer to respiratory care.
Completed dynamic SPECT only (MRI missing)	(Allencherril et al., 2019) patients	Patients excluded because they did not undergo MRI, primarily due unsatisfactory image quality.
Incomplete diagnostic evaluation (partial data available)	(Ciofani et al., 2021) patients	Patients with only fragmentary data, resulting in an incomplete diagnostic workup.

Note: The absolute contraindications include the presence of a left ventricular apical aneurysm and recurrent, life-threatening arrhythmias that preclude the safe performance of a stress test.

Table 2
Baseline clinical and demographic characteristics of included and excluded patients.

Indicator	Included patients	Excluded patients	p
	n-25	n-65	
Age, years	63.2 (±11.7)	64.4 (±10.7)	0.659
Male, n (%)	19 (76.0)	46 (70.8)	0.620
Hypertensive heart disease, n (%)	23 (92.0)	64 (98.5)	0.126
Smoking, n (%)	15 (60.0)	35 (53.9)	0.643
Body mass index, kg/m^2	29.3 (±4.3)	29.1 (±5.1)	0.872
Body surface area, m^2	2.0 (±0.2)	2.0 (±0.3)	0.808
Type 2 diabetes mellitus, IGT, n (%)	8 (32.0)	36 (55.4)	**0.047**
Dyslipidemia, n (%)	20 (80.0)	50 (76.9)	0.753
Heredity, n (%)	10 (40.0)	30 (46.1)	0.642
History of angina pectoris, n (%)	4 (16.0)	10 (15.4)	0.943
History of prior MI, n (%)	2 (8.0)	5 (7.7)	0.961
Peripheral artery disease, n (%)	19 (76.0)	53 (81.5)	0.556
History of stroke, n (%)	1 (4.0)	8 (12.3)	0.239
AF, n (%)	3 (12.0)	8 (12.3)	0.968
Time from the onset of ACS symptoms, min	240.0 (160.0; 370.0)	220.0 (141.0; 440.0)	0.857
Thrombolytic therapy, n (%)	5 (20.0)	19 (29.2)	0.375
Laboratory data upon admission:			
GFR (CKD-EPI), ml/min/1.73 m2	63.6 (±13.1)	68.0 (±14.7)	0.195
Leukocyte count 10^9/L	10.3 (8.5; 13.8)	11.5 (9.7; 13.8)	0.195
Erythrocyte sedimentation rate, mm/h	12.0 (10.0; 19.0)	14.0 (8.0; 24.0)	0.963
C-reactive protein, mg/l	21.2 (13.0; 37.0)	20.8 (10.8; 38.0)	0.982
Platelet count 10^9/L	233.0 (184.0; 314.0)	221.0 (196.0; 281.0)	0.712
Glucose, mmol/l	9.4 (7.5; 12.1)	8.5 (7.4; 10.4)	0.567
Cholesterol, mmol/l	5.2 (±1.1)	5.3 (±1.2)	0.715
Triglycerides, mmol/l	1.7 (1.1; 3.0)	1.2 (0.7; 1.9)	0.455
Troponin I on admission, ng/ml	0.4 (0.1; 1.8)	0.4 (0.1; 2.6)	0.204
Peak Troponin I level, ng/ml	19.7 (6.1;25.0)	22.4 (11.1;25.0)	0.103
CPK - MV upon admission, units/l	31.0 (25.0;45.0)	36.5 (24.0;56.0)	0.480
Peak level of CPK - MV, units/l	143.8 (48.5;272.5)	150.1 (64.4;278.6)	0.463

(*continued on next page*)

Table 2 (*continued*)

Indicator	Included patients	Excluded patients	p
	n-25	n-65	
AHF grade according to the Killip scale upon admission:			
Killip I, n (%)	21 (84.0)	45 (69.2)	0.191
Killip II, n (%)	1 (4.0)	5 (7.7)	0.999
Killip III, n (%)	2 (8.0)	6 (9.2)	0.999
Killip IV, n (%)	2 (8.0)	8 (12.3)	0.720
P2Y12 inhibitors:			
Clopidogrel, n (%)	10 (40.0)	35 (52.3)	0.347
Ticagrelor, n (%)	13 (52.0)	30 (46.2)	0.645
Prasugrel, n (%)	2 (8.0)	0 (0.0)	0.481
Parameters for PCI:			
Residual coronary artery stenosis >50 %, n (%)	11 (44.0)	32 (49.2)	0.814
Direct stenting, n (%)	3 (12.0)	7 (10.8)	0.868
Infarction related coronary artery:			
Proximal LAD, n (%)	6 (24.0)	12 (18.5)	0.451
Mid LAD, n (%)	5 (20.0)	10 (15.4)	0.622
Distal LAD, n (%)	4 (16.0)	7 (10.8)	0.531
Diagonal branch of LAD, n (%)	3 (12.0)	4 (6.2)	0.394
Proximal LCx, n (%)	1 (4.0)	4 (6.2)	0.743
Obtuse marginal branch of LCx, n (%)	1 (4.0)	4 (6.2)	0.743
Proximal RCA, n (%)	3 (12.0)	14 (21.5)	0.292
Posterior descending artery, n (%)	2 (8.0)	10 (15.4)	0.324
Localization of infarction:			
Anteroseptal, n (%)	6 (24.0)	12 (18.5)	0.566
Anterior, n (%)	6 (24.0)	13 (20.0)	0.774
Anterolateral, n (%)	4 (16.0)	8 (12.3)	0.732
Lateral, n (%)	3 (12.0)	8 (12.3)	0.998
Inferior, n (%)	6 (24.0)	24 (36.9)	0.321
No-reflow treatment methods:			
Thrombaspiration, n (%)	12 (48.0)	26 (40.0)	0.634
Glycoprotein IIb/IIIa inhibitors, n (%)	16 (64.0)	27 (41.5)	0.064
Papaverine, n (%)	3 (12.0)	3 (4.6)	0.342
Nitroglycerine, n (%)	16 (64.0)	52 (80.0)	0.169
Adenosine, n (%)	3 (12.0)	5 (7.7)	0.482
TIMI blood flow after PCI before epinephrine administration:			
TIMI 0, n (%)	3 (12.0)	2 (4.6)	0.129
TIMI 1, n (%)	8 (32.0)	13 (20.0)	0.270
TIMI 2, n (%)	14 (56.0)	50 (76.9)	0.175
Outcomes:			
Achieving TIMI 3, n (%)	9 (36.0)	29 (44.6)	0.459
Hospital mortality, n (%)	1 (4.0)	5 (7.7)	0.923
MACE events within 30 days, n (%)	4 (16.0)	11 (16.9)	0.999

Variables are presented as mean and standard deviation (m ± SD) in case they are normally distributed, and as median (Me) and interquartile range (Q1; Q3) otherwise. Categorical variables were described by absolute and relative frequencies (%). Boldface denotes statistical significance.

Abbreviations: ACS – Acute Coronary Syndrome; AF – Atrial Fibrillation; AHF – Acute Heart Failure; CKD-EPI - Chronic Kidney Disease Epidemiology Collaboration Formula; CRP - C-Reactive Protein; ESR - Erythrocyte Sedimentation Rate; GFR – Glomerular Filtration Rate; IGT - Impaired Glucose Tolerance; LAD - Left Anterior Descending; LCX - Circumflex Coronary Artery; OM - obtuse marginal; PCI — Percutaneous Coronary Intervention; RCA – Right Coronary Artery; TIMI - Thrombolysis In Myocardial Infarction.

Data availability

Data will be made available on request.

References

Agostini, D., Roule, V., Nganoa, C., Roth, N., Baavour, R., Parienti, J.J., Beygui, F., Manrique, A., 2018 Jul. First validation of myocardial flow reserve assessed by dynamic 99mTc-sestamibi CZT-SPECT camera: head to head comparison with 15O-water PET and fractional flow reserve in patients with suspected coronary artery disease. The WATERDAY study. Eur. J. Nucl. Med. Mol. Imaging 45 (7), 1079–1090. https://doi.org/10.1007/s00259-018-3958-7.

Allencherril, J., Jneid, H., Atar, D., et al., 2019 Oct. Pathophysiology, diagnosis, and management of the no-reflow phenomenon. Cardiovasc. Drugs Ther. 33 (5), 589–597. https://doi.org/10.1007/s10557-019-06901-0.

Annibali, G., Scrocca, I., Aranzulla, T.C., et al., 2022. No-reflow phenomenon: a contemporary review. J. Clin. Med. 11 (8), 2233. https://doi.org/10.3390/jcm11082233.

Azzalini, L., Seth, M., Sukul, D., Arora, D.S., et al., 2022. Impact of left ventricular end-diastolic pressure on the outcomes of patients undergoing percutaneous coronary intervention. Am. J. Cardiol. 185, 107–114. https://doi.org/10.1016/j.amjcard.2022.09.007 (Epub 2022 Oct 7).

Ciofani, J.L., Allahwala, U.K., Scarsini, R., et al., 2021 Mar. No-reflow phenomenon in ST-segment elevation myocardial infarction: still the Achilles' heel of the

interventionalist. Futur. Cardiol. 17 (2), 383–397. https://doi.org/10.2217/fca-2020-0077.
ClinicalTrials.gov (n.d.). Efficiency and Safety of Intracoronary Epinephrine Administration in ST-Elevation Myocardial Infarction Patients With Refractory Coronary No-reflow. NCT04573751. Available at: https://clinicaltrials.gov/study/NCT04573751.
Dil, S.V., Vyshlov, E.V., Ryabov, V.V., 2022. Intracoronary epinephrine and verapamil in the refractory no-reflow phenomenon in patients with acute myocardial infarction. Cardiovasc. Ther. Prev. 21 (1), 2936. https://doi.org/10.15829/1728-8800-2022-2936.
Galli, M., Niccoli, G., De Maria, G., et al., 2024. Coronary microvascular obstruction and dysfunction in patients with acute myocardial infarction. Nat. Rev. Cardiol. 21 (5), 283–298. https://doi.org/10.1038/s41569-023-00953-4.
Gottdiener, J.S., Bednarz, J., Devereux, R., et al., 2004 Oct. American Society of Echocardiography. American Society of Echocardiography recommendations for use of echocardiog-raphy in clinical trials. J. Am. Soc. Echocardiogr. 17 (10), 1086–1119. https://doi.org/10.1016/j.echo.2004.07.013 (PMID: 15452478).
Hausenloy, D.J., Botker, H.E., Engstrom, T., et al., 2017. Targeting reperfusion injury in patients with ST-segment elevation myocardial infarction: trials and tribulations. Eur. Heart J. 38 (13), 935–941. https://doi.org/10.1093/eurheartj/ehw145.
Ibanez, B., James, S., Agewall, S., et al., 2018. 2017 ESC guidelines for the management of acute myocardial infarction in patients presenting with ST-segment elevation: the task force for the management of acute myocardial infarction in patients presenting with ST-segment elevation of the european society of cardiology (ESC). Eur. Heart J. 39, 119–177.
Kapur, N.K., O'Neill, W.W., 2019 Apr 1. Left ventricular end-diastolic pressure in acute myocardial infarction: a loaded target in need of unloading. Catheter. Cardiovasc. Interv. 93 (5), 910–911. https://doi.org/10.1002/ccd.28204.
Kaul, S., Methner, C., Cao, Z., Mishra, A., 2022 Sep 21. Mechanisms of the "no-reflow" phenomenon after acute myocardial infarction: potential role of Pericytes. JACC Basic Transl. Sci. 8 (2), 204–220. https://doi.org/10.1016/j.jacbts.2022.06.008.
Kloner, R.A., 2017. The importance of no-reflow/microvascular obstruction in the STEMI patient. Eur. Heart J. 38 (47), 3511–3513. https://doi.org/10.1093/eurheartj/ehx414.
van Kranenburg, M., Magro, M., Thiele, H., et al., 2014. Prognostic value of microvascular obstruction and infarct size, as measured by CMR in STEMI patients. JACC Cardiovasc. Imaging 7 (9), 930–939. https://doi.org/10.1016/j.jcmg.2014.05.010.
Liu, H., Wu, J., Miller, E.J., Liu, C., et al., 2021 Aug. Diagnostic accuracy of stress-only myocardial perfusion SPECT improved by deep learning. Eur. J. Nucl. Med. Mol. Imaging 48 (9), 2793–2800. https://doi.org/10.1007/s00259-021-05202-9.
Nagueh, S.F., Smiseth, O.A., Appleton, C.P., Byrd 3rd, B.F., Dokainish, H., Edvardsen, T., Flachskampf, F.A., Gillebert, T.C., Klein, A.L., Lancellotti, P., Marino, P., Oh, J.K., Popescu, B.A., Waggoner, A.D., 2016 Apr. Recommendations for the evaluation of left ventricular diastolic function by echocardiography: an update from the American Society of Echocardiography and the European Association of Cardiovascular Imaging. J. Am. Soc. Echocardiogr. 29 (4), 277–314. https://doi.org/10.1016/j.echo.2016.01.011.
Otaki, Y., Manabe, O., Miller, R.J.H., Manrique, A., Nganoa, C., Roth, N., Berman, D.S., Germano, G., Slomka, P.J., Agostini, D., 2021 Aug. Quantification of myocardial blood flow by CZT-SPECT with motion correction and comparison with 15O-water PET. J. Nucl. Cardiol. 28 (4), 1477–1486. https://doi.org/10.1007/s12350-019-01854-1.
Reinstadler, S.J., Stiermaier, T., Reindl, M., et al., 2019. Intramyocardial haemorrhage and prognosis after ST-elevation myocardial infarction. Eur. Heart J. Cardiovasc. Imaging 20 (2), 138–146. https://doi.org/10.1093/ehjci/jey101.
Robbers, L.F., Eerenberg, E.S., Teunissen, P.F., et al., 2013. Magnetic resonance imaging-defined areas of microvascular obstruction after acute myocardial infarction represent microvascular destruction and haemorrhage. Eur. Heart J. 34 (30), 2346–2353. https://doi.org/10.1093/eurheartj/eht100.
Ryabov, V.V., Popov, S.V., Vyshlov, E.V., et al., 2023. Reperfusion cardiac injury. The role of microvascular obstruction. Sib. J. Clin. Exp. Med. 38 (2), 14–22. https://doi.org/10.29001/2073-8552-2023-39-2-14-22.
Ryabov, V.V., Vyshlov, E.V., Maslov, L.N., et al., 2024a. The role of microvascular obstruction and intra-myocardial hemorrhage in reperfusion cardiac injury. Analysis of clinical data. Rev. Cardiovasc. Med. 25 (3), 105. https://doi.org/10.31083/j.rcm2503105.
Ryabov, V.V., Dil, S.V., Vyshlov, E.V., et al., 2024b. Efficiency and safety of intracoronary epinephrine administration in patients with ST-elevation myocardial infarction with refractory coronary no-reflow. Am. J. Cardiol. 226, 118–127. https://doi.org/10.1016/j.amjcard.2024.07.011.
Scarsini, R., Shanmuganathan, M., De Maria, G.L., Borlotti, A., Kotronias, R.A., Burrage, M.K., Terentes-Printzios, D., Langrish, J., Lucking, A., Fahrni, G., Cuculi, F., Ribichini, F., Choudhury, R.P., Kharbanda, R., Ferreira, V.M., Channon, K.M., Banning, A.P., OxAMI study investigators, 2021. Coronary microvascular dysfunction assessed by pressure wire and CMR after STEMI predicts long-term outcomes. JACC Cardiovasc. Imaging 14 (10), 1948–1959. https://doi.org/10.1016/j.jcmg.2021.02.023.
Vorobeva, D.A., Ryabov, V.V., Lugacheva, J.G., et al., 2022. Relationships between indicators of prothrombotic activity and coronary microvascular dysfunction in patients with myocardial infarction with obstructive and non-obstructive coronary artery disease. BMC Cardiovasc. Disord. 22, 530. https://doi.org/10.1186/s12872-022-02985-z.
Vyshlov, E.V., Dil, S.V., Baev, A.E., et al., 2024. Intracoronary Administration of Epinephrine in the refractory no-reflow phenomenon in patients with acute myocardial infarction. Kardiologiia 64 (6), 34–42 (In Russ.). 10.18087/cardio.2024.6.n2493.
de Waha, S., Patel, M.R., Granger, C.B., et al., 2017. Relationship between microvascular obstruction and adverse events following primary percutaneous coronary intervention for ST-segment elevation myocardial infarction: an individual patient data pooled analysis from seven randomized trials. Eur. Heart J. 38 (47), 3502–3510. https://doi.org/10.1093/eurheartj/ehx414.